Invited Review
Chinese Science Bulletin
SPECIAL ISSUE
Basic Plasma Processes in Solar-Terrestrial Activities
April 2012 Vol.57 No.12: 1369–1374
doi: 10.1007/s11434-012-5045-y

Recent progresses in theoretical studies and satellite observations for collisionless magnetic reconnection

WANG XiaoGang[1*], XIAO ChiJie[1], PU ZuYin[2] & WANG JiaQi[3]

[1] *School of Physics and State Key Laboratory of Nuclear Physics & Technology, Peking University, Beijing 100871, China;*
[2] *School of Earth and Space Sciences, Peking University, Beijing 100871, China;*
[3] *College of Physical Science and Technology, Sichuan University, Chengdu 610064, China*

Received November 4, 2011; accepted December 27, 2011

As an essential mechanism in large scale fast magnetic energy releases and field reconfigurations processes in space, astrophysical, and laboratory plasmas, magnetic reconnection, particularly collisionless magnetic reconnection, has been studied for more than 65 years. Many progresses have been achieved in recent years and basic features of the process have been well understood, largely due to more and more satellite observation data available in the last decade. However, a few outstanding issues are still remained unresolved. We in the paper review the development of collisionless magnetic reconnection studies and major achievements in recent years, and also briefly discuss the open questions remained to be answered in studies of collisionless magnetic reconnection.

magnetic reconnection, fast reconnection rate, waves in two-fluid models, out-of-plane magnetic component

Citation: Wang X G, Xiao C J, Pu Z Y, et al. Recent progresses in theoretical studies and satellite observations for collisionless magnetic reconnection. Chin Sci Bull, 2012, 57: 1369–1374, doi: 10.1007/s11434-012-5045-y

Magnetic reconnection is thought an essential mechanism in many plasma physics processes in space, laboratory, and astrophysical objects, related to configurations relaxation and fast release of magnetic field and energy, observed in laboratory experiments and satellites observations and studied in numerical simulations and theoretical analysis [1].

The concept of magnetic reconnection was first proposed as a process of oppositely directed magnetic field lines merging and annihilated at a magnetic null, in an effort to understand the solar flare phenomenon [2]. The idea further developed by Sweet [3] and Parker [4] into a neutral line merging model with the electrical resistivity η as the dissipation mechanism, which led to a reconnection rate of $S^{-1/2}\sim\eta^{1/2}$, where the Lundquist number $S\equiv\tau_R/\tau_A$ with the resistive diffusion time $\tau_R\sim\eta^{-1}$, and the Alfvén time $\tau_A=L/V_A$, $V_A = B/\sqrt{4\pi n m_i}$ the Alfvén speed and L the typical scale length of the magnetohydrodynamics (MHD) region. It has then become a fundamental model in magnetic reconnection studies. Nevertheless, the Sweet-Parker reconnection rate is on the order of square root of the electrical resistivity. Due to the low collisionality in space and solar plasmas, the rate is too slow to be counted for fast events such as solar flares. Another model was then proposed by Petschek, with a fast driven and an X-point geometry, to solve the problem [5]. It was claimed in the Petschek model that a fast reconnection rate could be almost on the order of logarithm of resistivity, much faster than the Sweet-Parker rate. It was however found latterly that in high resolution simulations, the X-point geometry could not be realized in high Lundquist number regime of $S\geqslant 10^4$ [6]. And in the low Lundquist number regime ($S<10^3$), Petschek reconnection rate and Sweet-Parker reconnection rate would be more or less on the same order.

On the other hand, collisionless mechanisms such as the finite Larmor radius (FLR) effect rather than collisional

*Corresponding author (email: xgwang@pku.edu.cn)

resistivity in Sweet-Parker and Petschek models were introduced to resolve the current singularity on the reconnection neutral line. In the collisionless magnetic reconnection theory developed in early years, the effect of the electron FLR $\rho_{ce} = V_e / \Omega_{ce}$, with $V_e = \sqrt{T_e / m_e}$ being the electron thermal velocity and $\Omega_{ce} = eB / m_e c$ being the electron gyro-frequency, was taken into account to get rise to the growth rate of an electron tearing mode [7,8]:

$$\gamma = \frac{V_e}{L}\left(\frac{\rho_{ce}}{L}\right)^{3/2}\left[1+\frac{T_i}{T_e}\right](1-k^2L^2).$$

Unfortunately, even for high beta plasmas, the growth rate is still too slow to be compared with the time scale of fast events such as solar flares and magnetospheric substorm onsets, due to the fact of $\rho_{ce} / L << 1$. For example, in magnetotail plasmas where beta is on the order of unity with $V_e \sim V_A$, the typical ratio of $\rho_{ce} / L < 10^{-2}$ leading to $\gamma < 10^{-3} V_{the} / L \sim 10^{-3}\omega_A$, $\omega_A \equiv 1/\tau_A$.

When other mechanisms such as the anomalous resistivity and/or hyperresistivity (also called anomalous electron viscosity) were suggested [9–11], the dynamics in the ion inertial range $d_i = c/\omega_{pi}$, c the speed of light and $\omega_{pi} = (4\pi ne^2 / m_i)$ the ion plasma frequency, attracted more attentions in 1990s [12–15]. A fast growth rate in the sub-Alfvénic regime for nonlinear kink-tearing modes in tokamak plasmas was found scaled as $\gamma / \omega_A \sim (\omega_A / \Omega_{ci})^{1/2} \sim (d_i / L)^{1/2}$ [14,15]. In high beta plasmas without the guide field in the reconnection region, such a fast reconnection rate has been thought resulting from the Hall effect in the general Ohm's law.

Analytical and numerical advances in collisionless magnetic reconnection based on Hall MHD and other similar models such as the hybrid model [16–25] have been largely driven by satellite observations in the last decade [26–34]. We in this paper review these developments and discuss outstanding issues raised by satellite observations and to be answered by theory and simulation. In the next sections, we describe and analyze the significant developments in theoretical predictions and satellite observations of collisionless magnetic reconnection, particularly the major features of Hall effects such as typical length scales, the fast reconnection rate, whistler waves, and the quadrupolar "out-of-plane" magnetic field. The paper is then concluded in a summary and discussions.

1 The typical scale lengths of Hall effect

The major features of collisionless reconnection, particularly a fast reconnection rate in the sub-Alfvénic regime, a quadrupolar structure of the "out-of-plane" magnetic field, whistler waves in the reconnection region, and typical length scales have been taken as clear evidences of Hall effects in the reconnection process. We now discuss the major features of the Hall effects in this and following sections.

The Hall effect was first reported in 1879 by Edwin Hall as a phenomenon that an electric field would be established while a current perpendicularly flew through a magnetic field. Clearly, the basic physical mechanism of the effect is the separation of the electron motion from the ion in a small ion gyroradius scale. If the typical ion speed is Alfvénic, the corresponding ion gyroradius then should be the Alfvénic gyroradius $V_A / \Omega_{ci} = d_i$, i.e. the ion inertial length.

The ion inertial scale of the Hall effect can be clearly seen in the generalized Ohm's law in its dimensionless form:

$$\boldsymbol{E} + \boldsymbol{v} \times \boldsymbol{B} = \frac{1}{S}\boldsymbol{J} + \frac{d_e^2}{n}\frac{\mathrm{d}\boldsymbol{J}}{\mathrm{d}t} + \frac{d_i}{n}(\boldsymbol{J} \times \boldsymbol{B} - \beta_e \nabla p_e), \qquad (1)$$

where the dimensional translations are

$$\frac{c\boldsymbol{E}}{B_0 V_{A0}} \to \boldsymbol{E},\ \frac{\boldsymbol{B}}{B_0} \to \boldsymbol{B},\ \frac{\boldsymbol{v}}{V_{A0}} \to \boldsymbol{v},\ \frac{4\pi a \boldsymbol{J}}{cB_0} \to \boldsymbol{J},$$

$$\frac{n}{n_0} \to n,\ \frac{p_e}{p_0} \to p_e,\ \omega_{A0} t \to t,$$

as well as $a\nabla \to \nabla$; with the B_0, a, n_0, and p_0 being the characteristic magnetic field strength, length scale, plasma density, and electron pressure respectively, and $\omega_{A0} = V_{A0} / a$ with V_{A0} being the Alfvén speed calculated from B_0 and n_0; also other dimensionless parameters are the Lindquist number $S \equiv \omega_{A0}\tau_R$ (the magnetic diffusion time $\tau_R \equiv \eta c^2 / 4\pi a^2$), and the characteristic electron beta $\beta_e = 8\pi p_0 / B_0^2$.

In eq. (1) $d_i \boldsymbol{J} \times \boldsymbol{B} / n$ is the Hall electrical field term. The left-hand-side of equation can be reduced to $\partial\psi / \partial t + \boldsymbol{v} \cdot \nabla\psi$ in a two-dimensional (2D) approximation [19]. The dimensionless reconnection rate $\partial\psi / \partial t$ scaled by $V_A B_{in}$ can then be measured by the ratio of V_{rec}/V_A, where ψ is the reconnected flux, B_{in} is the merging (reconnecting) magnetic field, and V_{rec} is the merging velocity. From the continuity $V_{rec} = (\Delta / l) V_A$, with Δ being the width and l being the length of the reconnection layer [4], shown in Figure 1, the rate can also be simply determined by the ratio of the layer width to the length ~Δ / l. If the ions are Alfvénic, the reconnection layer width should have a d_i scaling. It was then found in a nonlinear dynamics model for sawtooth crashes in tokamak plasmas that the layer width $\Delta \sim (\omega_A / \Omega_{ci}) w$ indeed had the d_i scaling, with $\omega_A / \Omega_{ci} = d_i / r_s$, where $r_s \sim L$ is the radius of the m/n=1 surface, and w is the m/n=1 island width. The scaling has then also been reported in observations and many other theoretical and numerical studies [16–33].

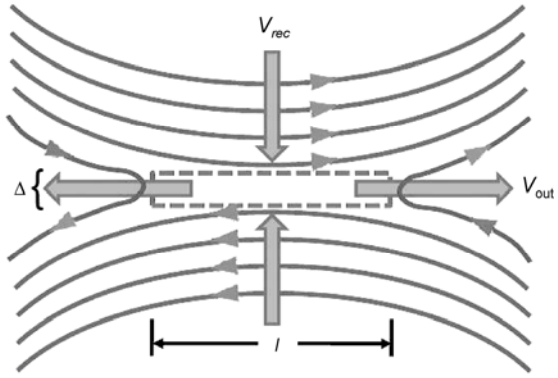

Figure 1 A sketch of the reconnection layer, with V_{rec} the reconnection rate, V_{out}~V_A the out-flow velocity, Δ the layer width and l the layer length.

Study for the reconnection layer length however took much more efforts. In the nonlinear dynamics model for the sawtooth, the length of the reconnection range was calculated as $r_s\vartheta_0 \approx r_s(\omega_A/\Omega_{ci})^{1/2} \equiv (d_i r_s)^{1/2}$, where ϑ_0 the angle designating the location of the two tips of the m/n=1 island [14,15]. It was the first time that the reconnection layer length was found in a $d_i^{1/2}$ scaling. The result was then confirmed for Hall MHD reconnection in high beta plasmas with no guide-field [21,24]. It thus indicated that the collisionless magnetic reconnection rate should be in the $(d_i/r_s)^{1/2} \sim (d_i/L)^{1/2}$ scaling. Although there were no other predictions for the reconnection layer length, a different length scale could be obtained from a *universal* scaling of reconnection rate as $V_{rec} \approx 0.1V_A$, indicating a $\sim 10d_i$ layer length [16–18].

2 The fast reconnection rate

To measure the scales, particularly the reconnection layer length, is a great challenge to experiments and satellite observations. On the other hand however, dimensionless reconnection rate $\sim \Delta/l$ can be measured to indirectly test the related theories or the length scale. Moreover, to understand the fast solar and magnetosphere events such as flares and substorm onsets is the initial motivation for magnetic reconnection researches.

The universal scaling was proposed with an argument that Hall MHD reconnection was mostly determined by the local ion dynamics, independent of global conditions [16]. Nevertheless, it was shown later that the boundary conditions could be important, in some cases even dominant, in reconnection processes and the merging speed V_{rec} under an asymptotic boundary perturbation could be as slow as a few percents of V_A, or even slower [19,21,22]. Furthermore, a reconnecting speed of $0.02V_A$ as predicted in [19] was reported in a Polar satellite observation at a subsolar magnetopause crossing [29]. The same result of the ~$0.02V_A$ reconnection rate was also found in a numerical simulation [22]. Certain events observed by the satellites Equator-S and Geotail also concluded that reconnection was determined by large-scale interactions between the solar wind and the magnetosphere, rather than by local conditions at the magnetopause [26]. On the other hand, a few Cluster observations in the magnetotail reported a much faster reconnection rate of ~0.07–0.30V_A [30,31].

To resolve the difference, Shay et al. tried to combine the two scalings, the d_i-dependent scaling and the *universal* scaling ~$0.1V_A$, together in a two-phase reconnection picture [23]. Starting from a thick current with a scale much wider than d_i, they found that the reconnection rate in the initial developmental phase was indeed "strongly dependent on the system size and presumably the dissipation mechanisms". In a later asymptotic phase however, the rate was "on the order of 0.1", independent of the system size and d_i. However extending our previous work further to the steady state, we found that the steady state fast reconnection rate of ~$0.1V_A$ was reduced as the perturbed boundary flow decreased, and for fixed boundary conditions, we again got the $(d_i/L)^{1/2}$ scaling of the reconnection rate [24]. In fact, the $(d_i/L)^{1/2}$ scaling model is consistent with the observations. For the subsolar magnetopause crossing on the dayside [28], the typical ratio of d_i/L~10^{-3}–10^{-4} leads to a reconnection rate of $(d_i/L)^{1/2}$~0.01–0.03, while in the magnetotail [30,31], the ratio of d_i/L~10^{-2} leads to a reconnection rate of $(d_i/L)^{1/2}$~0.1.

3 Whistler waves in the reconnection layer

The earlier theory of Hall MHD reconnection predicted that the fast rate of reconnection in collisionless plasmas was a direct consequence of the quadratic nature of the dispersion character of whistler waves, $\omega(\approx k^2 d_e^2 \Omega_{ce}) \sim k^2$ where $d_e = c/\omega_{pe}$ the electron skin depth ($\omega_{pe} = (4\pi n_0 e^2/m_e)^{1/2}$), which controlled the plasma dynamics at the small scales δ with $k \sim 1/\delta$ [16–18]. Nevertheless, later theoretical analysis showed that the whistler wave should be obliquely propagated with a much lower frequency of $\omega \approx k_{\|} k_{\perp} d_e^2 \Omega_{ce}$, where $k_{\|} << k_{\perp} \approx k \sim 1/\delta$ [19,20].

The dispersion relation can be derived from a reduced Hall MHD model in the 2D approximation [19]. In the dimensionless form, considering a Harris sheet equilibrium $\boldsymbol{B}_0 = \hat{x}\tanh z$, we write the magnetic field $\boldsymbol{B} = \hat{y}\times\nabla\psi + B_y\hat{y}$ and the plasma flow $\boldsymbol{v} = \hat{y}\times\nabla\phi + v_y\hat{y}$, and obtain $\boldsymbol{J} = \nabla^2\psi\hat{y} + \nabla B_y \times \hat{y}$. The equilibrium corresponds to $\phi_0 = v_{y0} = B_{y0} = 0$, and approximately $\psi_0 \approx z^2/2$ in the region of $|z| \leqslant 1$. Then we obtain $\nabla^2\psi_0 \approx 1$, $p_0 = p_{e0} = n_0 = 1 - \psi_0$. Linearizing the reduced Hall MHD model, we

obtain a set of reduced five-field linear equations [19]:

$$\frac{\partial \psi_1}{\partial t} = [\psi_0, \phi_1] + d_i[\psi_0, B_y], \tag{2}$$

$$\frac{\partial}{\partial t}\nabla^2\phi_1 = [\psi_0, \nabla^2\psi_1] + [\psi_0, p_{e1}] + [\psi_1, p_{e0}], \tag{3}$$

$$\frac{\partial p_{e1}}{\partial t} = [p_{e0}, \phi_1], \tag{4}$$

$$\frac{\partial B_y}{\partial t} = [\psi_0, v_y] - d_i\left([\psi_0, \nabla^2\psi_1] + [\psi_0, p_{e1}] + [\psi_1, p_{e0}]\right), \tag{5}$$

$$\frac{\partial^2 v_y}{\partial t} = [\psi_0, B_y], \tag{6}$$

where $[f, g] \equiv \hat{y}\cdot\nabla f \times \nabla g$ and $[\psi_0, \ ] = ik_{\parallel}V_A$ (V_A the local Alfvén speed). Under Fourier translations, we have the dispersion relation

$$\left(\frac{\omega}{k_{\parallel}V_A}\right)^4 \approx \left[2 + k^2 d_i^2\right]\left(\frac{\omega}{k_{\parallel}V_A}\right)^2 - 1. \tag{7}$$

Inside the reconnection layer, $kd_i > 1$, the dispersion relation (7) reduces to

$$\omega \approx k_{\parallel}kd_iV_A = k_{\parallel}kd_i^2\Omega_{ci} = k_{\parallel}kd_e^2\Omega_{ce}. \tag{8}$$

Clearly, this dispersion relation is for an obliquely propagated low frequency whistler mode.

Observationally whistler waves have indeed been detected in magnetic reconnection regions in magnetosphere plasmas where the plasma beta is on the order of unity [27,32,33]. The wave was found obliquely propagated with its wavevector nearly perpendicular to the ambient magnetic field, in a good agreement with the dispersion relation (8) [27]. The exact formula of the dispersion relation (8) was further confirmed recently by *k*-filter analysis for Cluster observation data [33]. It was also observed that the polarity of the wave was right-handed in the plane perpendicular to the ambient magnetic field, a typical electron mode feature [27,32]. This wave polarity property is however an open question to be further understood in theory.

4 The "out-of-plane" quadrupolar field

Studies on collisionless magnetic reconnection have also found that the electron convection in the 2D reconnection plane near the X-point due to the Hall effect can generate a characteristic quadrupolar pattern of the magnetic field perturbation B_y out of the "reconnection plane" (x, z), as shown in Figure 2 [24,27,29–31]. This so-called "Hall quadrupolar field" has been thought a typical signature and applied in satellite observations as a decisive criterion to identify fast

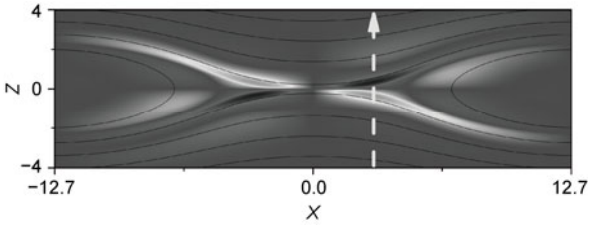

Figure 2 The out-of-plane quadrupolar field as observed in a satellite crossing.

reconnection processes [27,29–31]. However, the generation process of the quadrupolar magnetic field perturbation B_y has to be further understood analytically. Moreover, in a recent numerical study however, we found that with an out-of-plane shear flow, the quadrupolar magnetic field perturbation can also be generated even in "pure" 2D resistive reconnection [35]. The result then challenges the conventional understanding and satellite observations of the signature of collisionless magnetic reconnection evidences in space plasmas.

As in [35], a typical out-of-plane shear flow in the 2D model, $v_y(t=0) = V_S(z)$, can be written in the form of

$$V_S(z) = \begin{cases} -V_0 & z < -L_S, \\ V_0 \sin(\pi z / 2L_S) & -L_S < z < L_S, \\ V_0 & z > L_S, \end{cases} \tag{9a}$$

or

$$V_S(z) = \begin{cases} V_0[\cos(\pi z / L_S) + 1] & -L_S < z < L_S, \\ 0 & \text{Otherwise}, \end{cases} \tag{9b}$$

where the maximum speed of the shear flow V_0 is Alfvénic for space plasmas, and L_S is the flow shear length. The flow patterns of (9a) and (9b) are clearly the equilibrium solutions for the 2D model discussed above. From eq. (5) plus the equilibrium flow term $[\psi_1, v_{y0}]$ on its right-hand-side, near the neutral sheet z=0 we can approximately get a relation

$$\frac{\partial B_y}{\partial t} \approx B_{z1}v'_{y0}(z) = B_{z1}V'_S. \tag{10}$$

The in-plane magnetic perturbation near z=0, $B_{\text{in-plane}} \approx B_{z1}$, has an antisymmetry of $B_{z1}(x,z) = -B_{z1}(-x,z)$ about x=0 and a symmetry of $B_{z1}(x,z) = B_{z1}(x,-z)$ about z=0. On the other hand, the shear flow gradient has a symmetry of $V'_S(z) = V'_S(-z)$ in (9a) and an antisymmetry of $V'_S(z) = -V'_S(-z)$ in (9b), about z = 0. Then from the symmetry analysis of the right-hand-side of eq. (10), we can expect that the out-of-plane magnetic perturbation B_{y1} is either bipolar, i.e. antisymmetric about x=0 and symmetric about z=0, for the shear flow pattern (9a); or quadrupolar,

i.e. antisymmetric about both x=0 and z=0, for the shear flow pattern (9b). The numerical simulation shows in Figure 3 that the bipolar and quadrupolar magnetic perturbations generated by the shear flows (9a) and (9b) respectively can persist into the steady state nonlinear stage. The quadrupolar structure is very similar to that generated in Hall MHD reconnection (for example, that shown in Figure 2).

Thus, the issue should be raised particularly for those single satellite observations for reconnection, with only the signature of the out-of-plane field components. Since the shear flow is observed frequently in space plasmas, we also have to further study the effect of the shear flow on the Hall effect in collisionless plasmas.

5 Summary and discussion

We in the paper have reviewed the development of collisionless magnetic reconnection studies and major achievements in recent years, and also discussed the open questions and outstanding issues needed to be answered.

Collisionless magnetic reconnection in the Hall MHD approximation has been widely studied analytically and numerically. Although there are still certain issues to be resolved, such as the scaling of reconnection rate and layer length, a consensus is however reached for the major problem of collisionless magnetic reconnection, the fast reconnection rate. It has been found that the rate can be in the sub-Alfvénic regime of $V_{rec}/V_A \sim 0.01-0.3$, a result has been confirmed in recent satellite observations.

Another important result in collisionless reconnection studies is the whistler wave found in the reconnection region. It was thought the key cause of the fast reconnection rate. Together with more satellite data available in the recent decade, the basic picture has become more and more clear. It has been found theoretically and observationally that the wave is in the low frequency range between Alfvén and ion-cyclotron frequencies, and obliquely propagating with its wavenumber mostly perpendicular to the background magnetic field. However, the observed properties such as the right hand polarity and the electron mode feature are still open questions in theory to be answered.

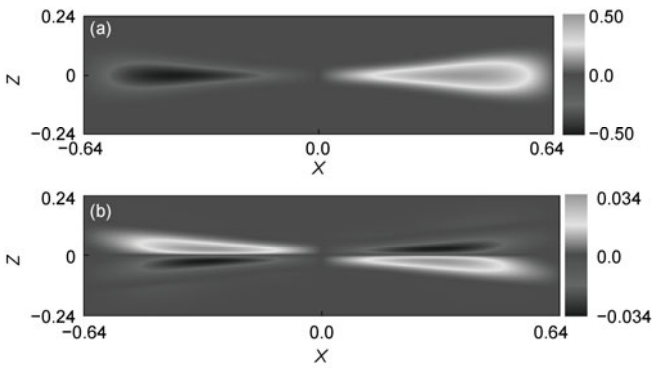

Figure 3 The out-of-plane quadrupolar field generated by (a) the shear flow of (9a) and (b) the shear flow of (9b).

The quadrupolar pattern of out-of-plane magnetic perturbations is taken as a decisive signature of collisionless reconnection. Nevertheless, it is found that shear flows can generate the similar patterns even in the resistive MHD frame. It thus challenges both observation and theory on how to identify a reconnection event since shear flows are constantly observed in space plasmas. Further study for shear flow effects in the Hall MHD model is then needed to address this issue.

Moreover, an open field in collisionless magnetic reconnection is the electron dynamics in the small scale of $\delta << d_i$ [36]. It was thought that this small scale should be on the order of the electron skin depth d_e, from the scaling of the electron inertial term $d_e^2 \mathrm{d}\boldsymbol{J}/n\mathrm{d}t$ in eq. (1) neglected in the Hall MHD model. However, recent laboratory experiments have shown a scale of the electron dynamics region one order of magnitude larger than d_e [37,38]. Thus, more efforts have to be done in this area.

The most important issue that hasn't been intensely explored is the three-dimensionality of reconnection. The progresses we have shown and discussed in this paper are mostly based on the 2D models. However, recent Cluster observations have revealed the three-dimensional structure of magnetic reconnection in the geo-magnetosphere plasmas [39–41]. The theory for the three-dimensional magnetic reconnection motivated by the observations then should be developed.

This work was supported by the National Natural Science Foundation of China (40731056, 10778613, 10675029, 10975012, 11005015, 40974104, 41104112) and Doctoral Fund of Ministry of Education of China (20090001110012).

1 Yamada M, Kulsrud R, Ji H. Magnetic reconnection. Rev Mod Phys, 2010, 82: 603–664
2 Giovanelli R G. A theory of chromospheric flares. Nature, 1946, 158: 81–82
3 Sweet P A. The neutral point theory of solar flares. In: Lehnert B, ed. Electro-magnetic Phenomena in Cosmical Physics. New York: Cambridge University Press, 1958
4 Parker E N. Sweet's mechanism for merging magnetic fields in conducting fluids. J Geophys Res, 1957, 62: 509–520
5 Petschek H G. Magnetic annihilation. In: Hess W N, ed. AAS-NASA Symposium on the Physics of Solar Flares, NASA Spec PublSp-50, 1964
6 Ma Z W, Ng C S, Wang X G, et al. Dynamics of current sheet formation and reconnection in two-dimensional coronal loops. Phys Plasmas, 1995, 2: 3184–3193
7 Laval G, Pellat R, Vuillemin M. Instabilites electromagnetiques des plasmas sans collisions. Plasma Phys Contr Fusion Res, 1966, 2: 259
8 Coppi B, Laval G, Pellat R. Dynamics of the geomagnetic tail. Phys Rev Lett, 1966, 16: 1207–1210
9 Coroniti F V. Space plasma turbulent dissipation: Reality or myth? Space Sci Rev, 1985, 42: 399–410
10 Aydemir A Y, Wiley J C, Ross D W. Toroidal studies of sawtooth oscillations in tokamaks. Phys Fluids B: Plasma Phys, 1989, 1: 774
11 Drake J F, Kleva R G. Collisionless reconnection and the sawtooth

crash. Phys Rev Lett, 1991, 66: 1458–1461
12 Aydemir A Y. Nonlinear studies of m=1 modes in high-temperature plasmas. Phys Fluids B: Plasma Phys, 1992, 4: 3469
13 Zakharov L, Rogers B, Migliuolo S. The theory of the early nonlinear stage of m=1 reconnection in tokamaks. Phys Fluids B: Plasma Phys, 1993, 5: 2498
14 Wang X, Bhattacharjee A. Nonlinear dynamics of the m = 1 instability and fast sawtooth collapse in high-temperature plasmas. Phys Rev Lett, 1993, 70: 1627–1630
15 Wang X, Bhattacharjee A. Nonlinear dynamics of the m = 1 kink-tearing instability in a modified magnetohydrodynamic model. Phys Plasmas, 1995, 2: 171
16 Shay M A, Drake J F. The role of electron dissipation on the rate of collisionless magnetic reconnection. Geophys Res Lett, 1998, 25: 3759–3762
17 Shay M A, Drake J F, Rogers B N, et al. Scaling of collisionless, magnetic reconnection for large systems. Geophys Res Lett, 1999, 26: 2163–2166
18 Shay M A, Drake J F, Rogers B N, et al. Alfvénic collisionless magnetic reconnection and the Hall term. J Geophys Res, 2001, 106: 3759–3772
19 Wang X, Bhattacharjee A, Ma Z W. Collisionless reconnection—Effects of Hall current and electron pressure gradient. J Geophys Res, 2000, 105: 27
20 Rogers B N, Denton R E, Drake J F, et al. Role of dispersive waves in collisionless magnetic reconnection. Phys Rev Lett, 2001. 87: 195004
21 Wang X, Bhattacharjee A, Ma Z W. Scaling of collisionless forced reconnection. Phys Rev Lett, 2001, 87: 265003
22 Dorelli J C. Effects of Hall electric fields on the saturation of forced antiparallel magnetic field merging. Phys Plasmas, 2003, 10: 3309
23 Shay M A, Drake J F, Swisdak M. The scaling of embedded collisionless reconnection. Phys Plasmas, 2004, 11: 2199
24 Wang X, Yang H A, Jin S P. Scalings of steady state Hall magnetohydrodynamic reconnection in high-beta plasmas. Phys Plasmas, 2006, 13: 060702
25 Huang C, Wang R S, Lu Q M, et al. Electron density hole and quadruple structure of B_y during collisionless magnetic reconnection. Chin Sci Bull, 2010, 55: 718–722
26 Phan T D, Kistler L M, Klecker B, et al. Extended magnetic reconnection at the Earth's magnetopause from detection of bi-directional jets. Nature, 2000, 404: 848–850
27 Deng X H, Matsumoto H. Rapid magnetic reconnection in the Earth's magnetosphere mediated by whistler waves. Nature, 2001, 410: 557–560
28 Scudder J D, Mozer F S, Maynard N C, et al. Fingerprints of collisionless reconnection at the separator. I, Ambipolar-Hall signatures. J Geophys Res, 2002, 107: 1294
29 Mozer F S, Bale S D, Phan T D. Evidence of diffusion regions at a subsolar magnetopause crossing. Phys Rev Lett, 2002, 89: 015002
30 Vaivads A, Khotyaintsev Y, Andre M, et al. Structure of the magnetic reconnection diffusion region from four-spacecraft observations. Phys Rev Lett, 2004. 93: 105001
31 Xiao C J, Pu Z Y, Wang X G, et al. A Cluster measurement of fast magnetic reconnection in the magnetotail. Geophys Res Lett, 2007, 34: L01101
32 Wei X H, Cao J B, Zhou G C, et al. Cluster observations of waves in the whistler frequency range associated with magnetic reconnection in the Earth's magnetotail. J Geophys Res, 2007, 112: A10225
33 Huang S Y, Zhou M, Sahraoui F, et al. Wave properties in the magnetic reconnection diffusion region with high β: Application of the k-filtering method to Cluster multispacecraft data. J Geophys Res, 2010, 115: A12211
34 Yan G Q, Shen C, Liu Z X, et al. Solar wind transport into magnetosphere caused by magnetic reconnection at high latitude magnetopause during northward IMF: Cluster-DSP conjunction observations. Sci China Ser E-Tech Sci, 2008, 51: 1677–1684
35 Wang J, Wang X, Xiao C. Out-of-plane bipolar and quadrupolar magnetic fields generated by shear flows in two-dimensional resistive reconnection. Phys Lett A, 2008, 372: 4614–4617
36 Lu Q M, Wang R S, Xie J L, et al. Electron dynamics in collisionless magnetic reconnection. Chin Sci Bull, 2011, 56: 1174–1181
37 Ren Y, Yamada M, Ji H, et al. Identification of the electron-diffusion region during magnetic reconnection in a laboratory plasma. Phys Rev Lett, 2008, 101: 85003
38 Zhong J, Li Y T, Wang X G, et al. Modelling loop-top X-ray source and reconnection outflows in solar flares with intense lasers. Nat Phys, 2010, 6: 984–987
39 Xiao C J, Wang X G, Pu Z Y, et al. In situ evidence for the structure of the magnetic null in a 3D reconnection event in the Earth's magnetotail. Nat Phys, 2006, 2: 478–483
40 Xiao C J, Wang X G, Pu Z Y, et al. Satellite observations of separator-line geometry of three-dimensional magnetic reconnection. Nat Phys, 2007, 3: 609–613
41 Pu Z Y, Zhang X G, Wang X G, et al. Global view of dayside magnetic reconnection with the dusk-dawn IMF orientation: A statistical study for Double Star and Cluster data. Geophys Res Lett, 2007, 34: L20101